Structural, electrical, and optical properties of thermally evaporated nanocrystalline PbTe films

Jianfei Wang,[1,a)] Juejun Hu,[1,b)] Xiaochen Sun,[1] Anuradha M. Agarwal,[1,c)] Lionel C. Kimerling,[1] Desmond R. Lim,[2] and R. A. Synowicki[3]
[1]*Microphotonics Center, Massachusetts Institute of Technology, Cambridge, Massachusetts 02139, USA*
[2]*DSO National Laboratories, Singapore 118230, Singapore*
[3]*Ellipsometry Services Laboratory, J. A. Woollam Co., Inc., Lincoln, Nebraska 68508, USA*

(Received 5 February 2008; accepted 19 June 2008; published online 4 September 2008)

Nanocrystalline PbTe films are deposited on different substrates at room temperature through thermal evaporation. The films are stoichiometric single-phase polycrystalline with (200) texture. Electrical properties of the films are analyzed in the framework of a grain boundary channel conduction model. The index of refraction and extinction coefficient of PbTe films are extracted from infrared spectroscopic ellipsometry measurement in the wavelength range of 2–8 μm, yielding an optical band gap of 0.386 eV and evidence for the presence of an Urbach band tail. The optical band gap is larger than the typical value for bulk material due to quantum confinement effect. © *2008 American Institute of Physics*. [DOI: 10.1063/1.2970163]

I. INTRODUCTION

The development of third generation infrared (IR) detector and focal plane array (FPA) devices is garnering a lot of interest around the world today. Key features of these devices include multicolor detection capability and two-dimensional arrays for hyperspectral imaging.[1] To date, HgCdTe has been the predominant material of choice for IR detection given its high performance, although the cost of HgCdTe photodetector devices remains extremely high due to expensive molecular beam epitaxy growth involved in device fabrication.[2,3] In addition, yield of HgCdTe FPA devices has been largely limited by the poor mechanical stability of HgCdTe alloys, especially in devices for long wavelength IR detection. Thus a low cost, robust, and multicolor detection technology still remains to be explored.

PbTe is a promising material candidate because of its superior chemical stability and the ease of film deposition. Band gap tunability can be achieved through alloying PbTe with SnTe.[4,5] Different deposition techniques have been employed for PbTe film deposition, including flash evaporation[6,7] and a hot-wall technique.[8] Single crystal PbTe and $Pb_{1-x}Sn_xTe$ have been studied for the fabrication of IR photodetectors[4] and long wavelength laser devices.[5] Boberl *et al.*[9] reported epitaxial PbTe detectors integrated with mid-IR filters and showed enhanced photoresponsivity at room temperature. High detectivity has also been obtained with polycrystalline PbTe films by Bode.[10] On the multispectral device design side, Sun *et al.*[11] have recently reported dual wavelength detection in a single pixel, through sandwiching multiple photoconductive layers in a one-dimensional photonic crystal structure. Our work leverages on such a multispectral pixel concept for IR detection using polycrystalline PbTe films, thereby significantly reducing the cost and improving device robustness, and thus a systematic study of the structural, electrical, and optical properties of polycrystalline PbTe films becomes essential for device design and performance evaluation.

In this paper we report structural, electrical, and optical properties of thermally evaporated PbTe films. We show that single phase stoichiometric PbTe films can be deposited using simple thermal evaporation from compound bulks suitable for mass production and cost reduction. Wavelength dispersive x-ray spectroscopy (WDS), x-ray diffraction (XRD), and atomic force microscope (AFM) are used to study the composition, phase structure, and morphology of the films, respectively. The dc electrical conductivity in the temperature range of 80–340 K is measured, and two distinct conduction mechanisms are identified in different temperature regimes. The index of refraction and extinction coefficient of the PbTe films were extracted from IR spectroscopic ellipsometry measurement in the wavelength range of 2–8 μm.

II. EXPERIMENT

Bulk PbTe of 99.999% purity from Alfa Aesar, Inc., is pulverized and used as the source material for thermal evaporation. Optically polished CaF_2 disks (Shandong Newphotons Science and Technology Co.), precleaned glass microscope slides (VWR International), and oxide coated Si wafers (4 in. Si wafers with 400 nm thermal oxide, Silicon Quest International) are used as the starting substrates. The thermal evaporation runs are carried out at a base pressure of 5×10^{-7} Torr. The substrates are held at room temperature throughout the depositions. The deposition rate is maintained at 5–7 Å/s.

The thickness of the films is measured using a Tencor P-10 surface profilometer. A JEOL JXA-733 superprobe equipped with WDS attachment is employed for film composition analysis. Film phase composition and structure are evaluated using XRD on a Rigaku powder diffractometer.

a)Electronic mail: wangjf05@mit.edu.
b)Electronic mail: hujuejun@mit.edu.
c)Electronic mail: anu@mit.edu.

 © 2008 American Institute of Physics

Author complimentary copy. Redistribution subject to AIP license or copyright, see http://jap.aip.org/jap/copyright.jsp

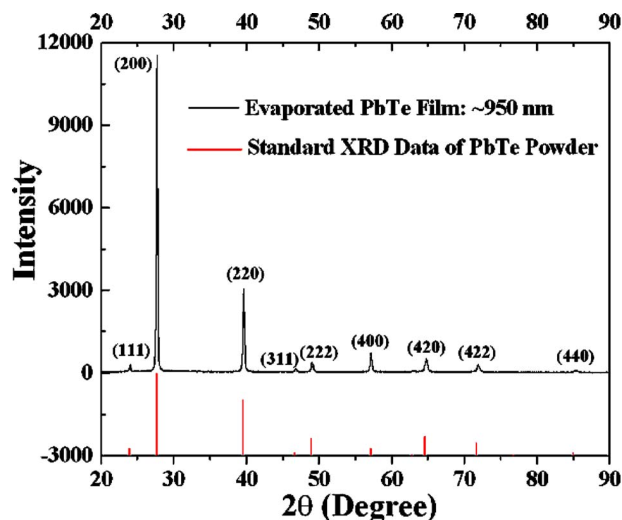

FIG. 1. (Color online) XRD spectrum of the thermally evaporated PbTe films on a glass substrate: the film is polycrystalline single fcc phase with (200) texture. Standard XRD data of PbTe powder sample from Ref. 12 are also shown at the bottom for comparison.

Grain size and surface roughness of the films are measured using a digital instruments nanoscope IIIa AFM.

Thermally evaporated tin electrodes are used as contacts for electrical conductivity and Hall measurements. In the conductivity measurement, current-voltage (*I-V*) curves are recorded using a Bio-Rad DL8000 digital DLTS system at temperatures from 80 to 340 K. Voltage is applied through a pair of metal probes and the current flowing through the two metal contacts is monitored. We observe linear *I-V* characteristics in the whole temperature range confirming Ohmic nature of the contact. Conductance at different temperatures is extracted by least-squares linear fit of *I-V* curves, and error of the measurement is estimated to be smaller than 1 pS. Hall measurement is performed at room temperature using the van der Pauw configuration in a magnetic field of $B=1$ T.

PbTe films evaporated on CaF_2 are used for optical property measurements given the IR transparency of CaF_2. Index of refraction and extinction coefficient of the PbTe films are extracted by fitting the amplitude ratio upon the reflection, the phase shift, and the transmission intensity data, all measured on a variable angle IR spectroscopic ellipsometer (IR-VASE of J. A. Woollam Co.) from 2 to 8 μm wavelength.

III. RESULTS AND DISCUSSION

A. Structural and morphological characterization

Profilometer measurement gives a film thickness of 950 nm $\pm 4\%$ across an entire substrate. Compositional analysis shows an atomic ratio of Pb to Te close to unity within the error of WDS measurement ($\sim 1\%$), indicating that the films are nearly stoichiometric.

An XRD spectrum of PbTe film deposited on a glass slide is shown in Fig. 1. The film contains a single face-centered-cubic (fcc) crystalline phase with a rocksalt structure. The diffraction peak intensities in the measured spectrum differ from those quoted from the standard PDF card,[11] indicating (200) texture in the film deposited on an amorphous glass substrate. Films on other substrates show a similar preferred orientation. The texture structure suggests that (200) is the preferred film growth orientation due to its low surface energy. This is consistent with the result of coevaporated PbTe thin films on glass substrates reported by Khairnar *et al.*,[13] which showed that (200) diffraction peak intensity varied with film thickness and substrate temperature during deposition.

Figure 2 shows the surface morphology of PbTe films on (a) a glass slide substrate and (b) a 400 nm SiO_2 coated Si substrate obtained by AFM. Both films show similar surface features: they have grain sizes in the range of 50–100 nm and rms surface roughness of 14–16 nm. The microstructural and morphological similarity between PbTe films deposited on different substrates is not coincidental and is indicative of the polycrystalline nature of PbTe films. From a device integration perspective, this roughness value has a negligible effect on the performance of photonic crystal cavities operating in mid-IR wavelengths according to Maskaly *et al.*[14,15]

B. Electrical characterization

The PbTe films show *p*-type conduction and carrier mobility of 53 $cm^2/V\ s$ from Hall measurement. The measured carrier concentration is 2.1×10^{17} cm^{-3} at room temperature.

To elucidate the conduction mechanism in thermally evaporated PbTe films, temperature dependence of the film dc electrical conductivity is measured and the result is plotted in Fig. 3. Qualitatively, our result gives a dc conductivity temperature dependence similar to that of In-doped PbTe films reported by Komissarova *et al.*[16] The conductivity exhibits thermally activated behavior in the high temperature

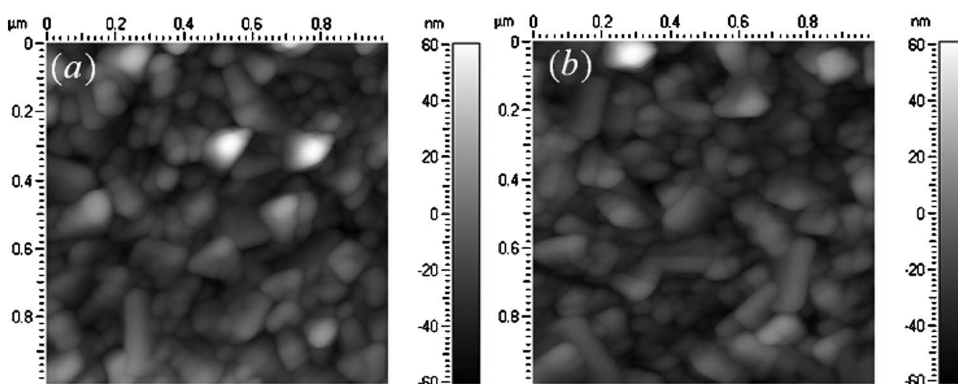

FIG. 2. AFM surface height images of thermally evaporated PbTe films on (a) a soda-lime glass substrate and (b) a Si substrate coated with 400 nm thermal oxide.

Author complimentary copy. Redistribution subject to AIP license or copyright, see http://jap.aip.org/jap/copyright.jsp

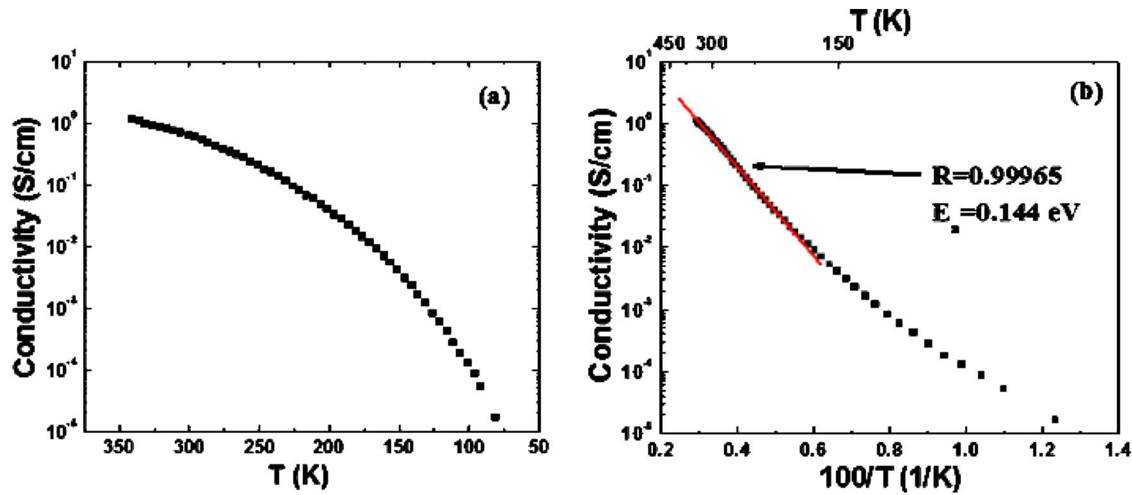

FIG. 3. (Color online) dc electrical conductivity of thermally evaporated PbTe films: (a) Conductivity data on a logarithm scale plotted as a function of temperature; lack of linear dependence in the plot suggests that electrical conduction in PbTe is not dominated by the percolation process. (b) Conductivity data plotted as a function of inverse temperature showing thermal activation nature of conduction at high temperature (>200 K) and a weaker temperature dependence at lower temperatures. The black dots are experimental data and the red solid line is linear curve fit of the data at high temperature (>200 K).

range and relatively weak temperature dependence at low temperatures, suggesting different regimes where distinct conduction mechanisms are dominant.

Several models have been previously proposed for electrical conductivity in PbTe and other chalcogenide films at different temperatures. Gudaev *et al.*[17] proposed a percolation model to explain the temperature dependence of electrical conductivity in polycrystalline chalcogenide films, which suggest that dc conductivity obeys the inverse Arrhenius law

$$\sigma \propto \exp(T/T'), \quad (1)$$

where T' is a constant determined by the percolation parameters. However, such an inverse Arrhenius temperature dependence is not observed in our films, as shown in Fig. 3(a). Alternatively, conduction channels on the surface of crystal grains have been suggested to be the main electronic transport path in polycrystalline lead chalcogenide films.[18] In the framework of this theory, adsorbed oxygen or lattice defects lead to the formation of acceptor states in the grain boundaries. These acceptor states induce band bending on the surface of crystalline grains, and thus *p*-type conduction channels are formed on the grain surfaces. A schematic energy band diagram near a grain boundary is shown in Fig. 4. According to this model, dc electrical conductivity is thermally activated and can be described by an activation energy $E_a=(E_F-E_V)-E_S$, where (E_F-E_V) is the energy separation between the valence band edge and the Fermi level in crystalline PbTe grains and E_S corresponds to the band bending. Figure 3(b) shows the conductivity plotted as a function of inverse temperature, and in the high temperature range (approximately >200 K) the temperature dependence of conductivity can be well fitted with a single activation energy value of 0.144 eV. This model also agrees with our observation of *p*-type conduction in the films. However, since the exact carrier concentration and hence Fermi level in the grains are unknown, we cannot infer the value of band bending from the activation energy E_a.

In the low temperature range (<200 K) we can see clear deviation from the thermal activation model with weaker temperature dependence. Based on impedance spectroscopy measurement results, Komissarova *et al.*[16] inferred that tunneling transport through grain boundary barriers dictates the electrical properties of In-doped polycrystalline PbTe films at low temperature. Alternatively, hopping conduction between localized states in the mobility gap also exhibit weak temperature dependence characterized by the famous $T^{-1/x}$ law, where x is a constant greater than one depending on the system dimensionality and the form of density of states function near Fermi level.[19] Hopping conduction has been identified to be a major electronic transport mechanism in many chalcogenide materials, especially amorphous glasses.[20] In order for hopping transport to occur, two conditions need to be met: (1) Fermi level should be located within the mobility gap and (2) there should be nonvanishing density of states near Fermi level. Lattice defects in grains or near grain boundaries often lead to localized states in the mobility gap, possibly contributing to hopping conduction. The position of Fermi level in the films with respect to mobility edges, how-

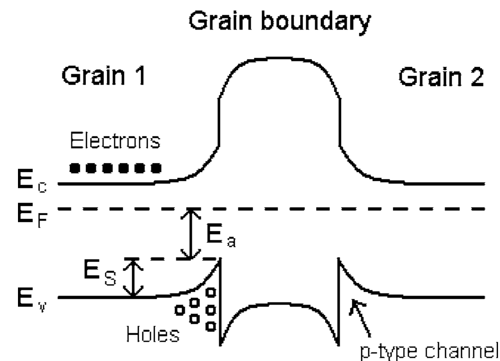

FIG. 4. Schematic energy band diagram near a grain boundary and the relevant energy points are: E_c the conduction band edge, E_v the valence band edge, E_F the Fermi level, E_S the band bending on the surface of a grain, and E_a the activation energy of electrical conduction according to the grain boundary conduction channel model.

Author complimentary copy. Redistribution subject to AIP license or copyright, see http://jap.aip.org/jap/copyright.jsp

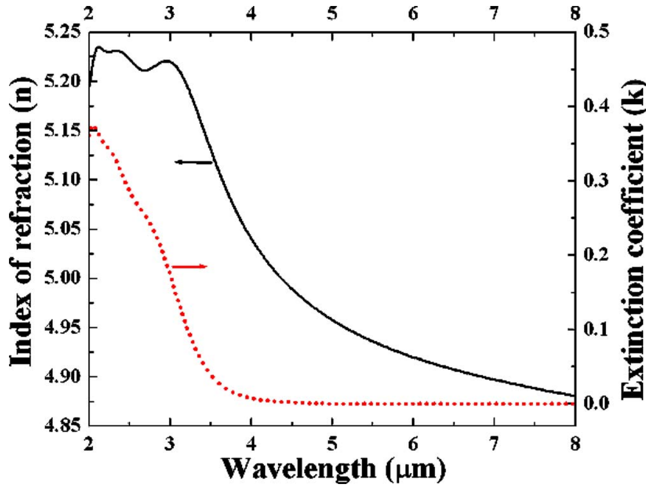

FIG. 5. (Color online) Refractive index and extinction coefficient of PbTe films are measured using IR ellipsometry.

ever, is a question for further investigation. More experimental efforts will be necessary to confirm the low temperature conduction mechanism in the films.

C. Optical characterization

Figure 5 shows the measured index of refraction and extinction coefficient of PbTe films at 2–8 μm wavelengths. Absorption coefficient α can be calculated from the extinction coefficient using the following relation:

$$\alpha = \frac{4 \times \pi \times k}{\lambda}, \quad (2)$$

where k is the extinction coefficient and λ is the wavelength, and is plotted in Fig. 6. Optical absorption due to electronic transition across the band gap in a direct gap semiconductor obeys

$$\alpha = \alpha_0 \times (h\upsilon - E_g)^{1/2}, \quad (3)$$

where α_0 is a constant determined by the joint density of states in the parabolic bands, $h\upsilon$ denotes incident photon energy, and E_g is the optical band gap energy.[21,22] Fitting of our experimental data using the formula (shown in Fig. 6, inset) yields an optical band gap of 0.386 eV. In addition to the optical transitions across the band gap, subband gap absorption is identified from 0.2 to 0.4 eV, where the absorption coefficient spans almost four orders of magnitude. This subband gap absorption is absent in single crystalline PbTe bulks and films and is attributed to Urbach band tail resulting from defect states in polycrystalline materials. Optical absorption by Urbach band tail can be described by the following formula:

$$\alpha \sim \exp\left(\frac{h\upsilon}{E_e}\right). \quad (4)$$

The energy E_e is a measure of structural disorder in the material, and the typical values of E_e in disordered semiconductors range between 0.05 and 0.08 eV.[23] E_e is fitted from the curve slope in Fig. 6 to be 0.056 eV, indicating disorderlike behavior of the PbTe films. Given the nanocrystalline nature of the films, we infer that structural defects in the grain boundaries account for the Urbach band tail.

It is worth pointing out that the fitted optical band gap energy in our nanocrystalline PbTe films is much larger than the bulk value of 0.31 eV due to quantum confinement effect.[6] As shown in Fig. 2, typical grain size of the film is in the range of 50–100 nm, much smaller than the exciton Bohr radius of 152 nm in PbTe. Therefore, the PbTe nanocrystallites in our films can lead to a strong three-dimensional quantum confinement effect, which may account for the optical band gap energy increase.[24] The quantum confinement effect in polycrystalline PbTe films has also been observed by Lawson *et al.*,[25] who reported increasing blueshift of photoconductivity onset as the average grain size of PbTe films decreases.

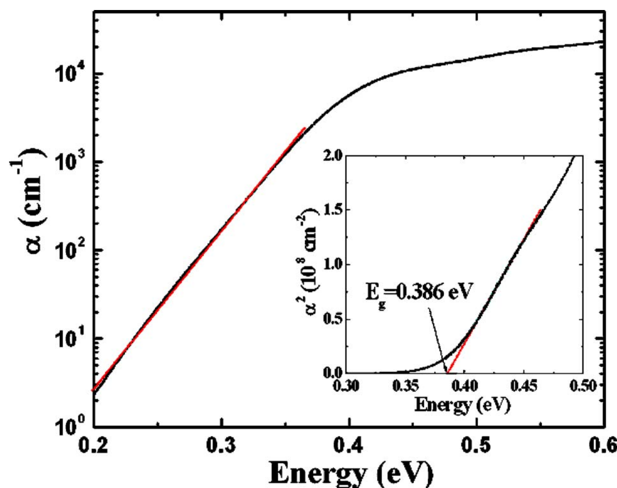

FIG. 6. (Color online) Absorption coefficient α of PbTe films as a function of photon energy. The inset shows α^2 plotted against photon energy for the determination of the optical band gap energy E_g.

IV. SUMMARY

In this paper, we present a systematic study on the structural, electrical, and optical properties of thermally evaporated PbTe films. As-deposited films are stoichiometric, single fcc phase polycrystals, and generally exhibit (200) texture on different substrates including amorphous glasses. The films feature grain sizes in the range of 50–100 nm and surface roughness of 14–16 nm. We experimentally verify thermally activated behavior of p-type dc electrical conductivity in the films at temperatures higher than 200 K, and such temperature dependence is explained by the grain boundary channel conduction model. At reduced temperature the electrical conductivity exhibits weaker temperature dependence possibly due to hopping or tunneling transport. The refractive index and extinction coefficient of the films are measured at IR wavelengths, and the optical band gap energy is determined to be 0.386 eV using a direct transition model, larger than the bulk value reported in single-crystalline PbTe. Such a band gap increase is pertinent to the nanocrystalline nature of the films and is a consequence of the ensuing quantum confinement effect. We also observe subband gap ab-

Author complimentary copy. Redistribution subject to AIP license or copyright, see http://jap.aip.org/jap/copyright.jsp

sorption due to an Urbach band tail, indicating the presence of defect states possibly arising from the disordered regions in the grain boundaries.

ACKNOWLEDGMENTS

This work is supported by the DSO National Laboratories in Singapore. The authors would like to thank Dr. Nilanjan Chatterjee and Dr. Mayank Bulsara for their technical assistance in WDS and AFM measurements. The authors also acknowledge the Center for Materials Science and Engineering at MIT for characterization facilities.

[1] A. Rogalski, Prog. Quantum Electron. **27**, 59 (2003).
[2] S. M. Johnson, W. A. Radforda, A. A. Buell, M. F. Vilela, J. M. Peterson, J. J. Franklin, R. E. Bornfreund, A. C. Childs, G. M. Venzor, M. D. Newton, E. P. G. Smith, L. M. Ruzicka, G. K. Pierce, and D. D. Lofgreen, Proc. SPIE **5732**, 250 (2005).
[3] E. P. G. Smith, L. T. Pham, G. M. Venzor, E. M. Norton, M. D. Newton, P. M. Goetz, V. K. Randall, A. M. Gallagher, G. K. Pierce, E. A. Patten, R. A. Coussa, K. Kosai, W. A. Radford, L. M. Giegerich, J. M. Edwards, S. M. Johnson, S. T. Baur, J. A. Roth, B. Nosho, T. J. De Lyon, J. E. Jensen, and R. E. Longshore, J. Electron. Mater. **33**, 509 (2004).
[4] I. Melngailis and T. C. Harman, *Semiconductors and Semimetals* (Academic, New York, 1970), Vol. 5, p. 111.
[5] T. C. Harman and I. Melngailis, *Applied Solid State Science* (Academic, New York, 1974) Vol. 4, p. 1.
[6] T. S. Moss, Proc. IRE **43**, 1869 (1955).
[7] F. S. Terra, M. Abdel-Rafea, and M. Monir, J. Mater. Sci.: Mater. Electron. **12**, 561 (2001).
[8] Y. A. Ugai, A. M. Samoylov, M. K. Sharov, and A. V. Tadeev, Thin Solid Films **336**, 196 (1998).
[9] M. Boberl, T. Fromherz, J. Roither, G. Pillwein, G. Springholz, and W. Heiss, Appl. Phys. Lett. **88**, 041105 (2006).
[10] D. E. Bode, Phys. Thin Films **3**, 275 (1966).
[11] X. Sun, J. Hu, C. Hong, J. F. Viens, X. M. Duan, R. Das, A. M. Agarwal, and L. C. Kimerling, Appl. Phys. Lett. **89**, 223522 (2006).
[12] Powder Diffraction File (PDF) Card No. 781905.
[13] U. P. Khairnar, P. H. Pawar, and G. P. Bhavsar, Cryst. Res. Technol. **37**, 1293 (2002).
[14] K. R. Maskaly, W. C. Carter, R. D. Averitt, and J. L. Maxwell, Opt. Express **13**, 8380 (2005).
[15] K. R. Maskaly, G. R. Maskaly, W. C. Carter, and J. L. Maxwell, Opt. Lett. **29**, 2791 (2004).
[16] T. Komissarova, D. Khokhlov, L. Ryabova, Z. Dashevsky, and V. Kasiyan, Phys. Rev. B **75**, 195326 (2007).
[17] O. A. Gudaev, V. K. Malinovsky, E. E. Paul, and V. A. Treshikhin, Solid State Commun. **74**, 1169 (1990).
[18] Z. Dashevsky, *Handbook of Semiconductor Nanostructures and Nanodevices* (American Scientific Publishers, Stevenson Ranch, 2006), Vol. 2, p. 335.
[19] N. F. Mott, Philos. Mag. **19**, 835 (1969).
[20] J. Hu, X. Sun, A. M. Agarwal, J. Viens, L. C. Kimerling, L. Petit, N. Carlie, K. C. Richardson, T. Anderson, J. Choi, and M. Richardson, J. Appl. Phys. **101**, 063520 (2007).
[21] V. Srikant and D. R. Clarke, J. Appl. Phys. **83**, 5447 (1998).
[22] D. B. Haddad, J. S. Thakur, V. M. Naik, G. W. Auner, R. Naik, and L. E. Wenger, MRS Symposia Proceedings No. 743 (Materials Research Society, Pittsburgh, 2003), p. L11.22.1.
[23] J. Tauc, *Amorphous and Liquid Semiconductors* (Plenum, London, 1974), p. 159.
[24] A. L. Rogach, A. Eychmuller, S. G. Hickey, and S. V. Kershaw, Small **3**, 536 (2007).
[25] W. D. Lawson, F. A. Smith, and A. S. Young, J. Electrochem. Soc. **107**, 206 (1960).

Author complimentary copy. Redistribution subject to AIP license or copyright, see http://jap.aip.org/jap/copyright.jsp